Pattern formation caused by double quenches in binary polymer mixtures: Response of phase-separated structure to a second quench within a two-phase region

Hajime Tanaka
Department of Applied Physics and Applied Mechanics, Institute of Industrial Science, University of Tokyo, Minato-ku, Tokyo 106, Japan
(Received 25 September 1992)

Here we demonstrate the evolution of an unusual phase-separated pattern caused by a double quench: a first quench from a one-phase to a two-phase region and a subsequent second quench within the two-phase region. The resulting pattern evolution strongly depends upon the type of a double-quench sequence. A *deeper* second quench causes a level structure, while a *shallower* one causes a long-range interface instability coming from a mismatch in the local volume-surface ratio. The response of a domain structure to a second quench is qualitatively discussed on the basis of the phase diagram and existing theories for the coarsening dynamics of usual phase separation.

PACS number(s): 64.75.+g, 61.25.Hq, 64.70.−p

Generally, dynamics and morphology of phase separation are strongly dependent on a quench condition, which gives a final equilibrium free energy. Thus a quench condition including the change in composition, temperature, and pressure of a mixture is one of the key factors dominating the phase-separation behavior. So far most of the studies on phase-separation phenomena have been limited to an ordering process accompanied by a single quench from a one-phase to a two-phase region [1,2]. For single quenches, phase-separation phenomena are divided into nucleation growth (NG) and spinodal decomposition (SD) in the mean-field picture [1–3], depending upon quench conditions. There is a possibility that new types of phase-separated patterns are caused by unusual quench conditions. From this standpoint, the problem related to relaxation of a nonequilibrium state or fluctuation under special quench conditions has been studied by some researchers, and so far classified into the following three cases [1]: (i) A temperature or pressure quench in a stable, one-phase region [4,5]; (ii) a double quench. The system is first quenched from a one-phase to a two-phase region, and then subsequently back to the one-phase region [6,7]; and (iii) periodic variations of temperature which bring the system alternatively below and above the phase-separation point. This periodic spinodal decomposition was predicted by Onuki [8–10] and then experimentally studied [11,12].

Here we focus our attention on another kind of a double temperature quench, which consists of a first quench from a one-phase to a two-phase region and a subsequent second quench *within the two-phase region*. The second quench can further be grouped into two kinds: a deeper quench and a shallower quench. These kinds of double quenches are largely unexplored [13–15], although interface stability under double-quench conditions has been theoretically studied [13]. In this paper we describe examples of pattern evolution caused by double quenches within the two-phase region and discuss the mechanism of pattern evolution, including the interface stability of an original domain structure against a second quench.

The samples used where a binary mixture of polystyrene (PS) and poly(vinyl methyl ether) (PVME) and that of PVME and water. The weight-average molecular weights of PS and PVME were 20 000 and 98 200, respectively. Both systems have lower critical solution temperature type phase diagrams. The symmetric compositions for PS-PVME and PVME-water mixtures were 60 wt. % PVME and 7 wt. % PVME, respectively. The temperature of a sample was controlled by a hot stage (Linkam TH-600 RMS). The maximum rate of the temperature change was 1.5 °C/s. The phase-separated morphology was observed by phase-contrast microscopy. A double-quench experiment was performed as follows: A mixture was brought from the stable, one-phase region to the two-phase region by a first temperature jump from T_0 to T_1 across the binodal temperature T_{bn}, and consequently the system separates into two macroscopic phases with time. After a certain period (Δt), the temperature of the system is again changed from T_1 to T_2 within the two-phase region by a second quench. Then the pattern evolution after this second quench is studied. This double quench is characterized by the following quantities: $\Delta T_1 = T_1 - T_{bn}$, Δt, $\Delta T_2 = T_2 - T_{bn}$, T_0, and T_{bn}. Here we express a double quench by these parameters as $(\Delta T_1, \Delta t, \Delta T_2)(T_0, T_{bn})$.

First we describe experimental results for a double quench composed of a first quench into the unstable region and a subsequent *deeper* quench. Figure 1 shows pattern formation in a PS-PVME (50-50) (50 wt. % PS, 50 wt. % PVME) caused by a double quench (6.8 °C, 600 s, 21.4 °C) (163.0 °C, 168.0 °C). After the second deeper quench, SD-like phase separation occurs in the two original, coexisting phases. The initial periodically modulated structure, which is rather difficult to resolve by optical microscopy [Figs. 1(a) and (b)], transforms into a droplet-like morphology, reflecting the nonlinearity due to the composition asymmetry and also the dimensional crossover from three-dimensional (3D) to 2D. In the initial stage, phase separation probably proceeds almost independently in the two original phases. In the late stage, on the other hand, the large and small domains start to interact with each other through diffusion, and consequently small ones gradually evaporate from the vicinity

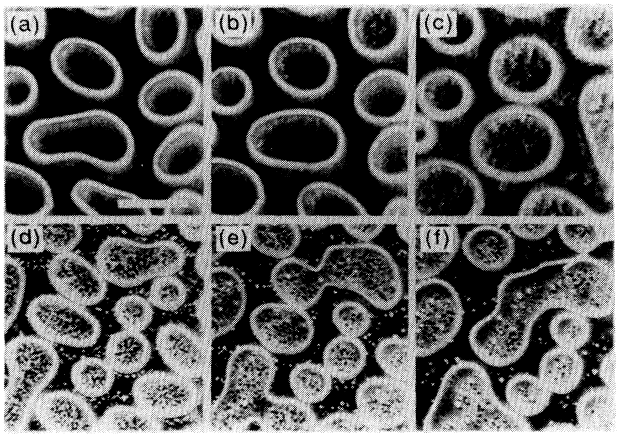

FIG. 1. Pattern evolution caused by a double quench (6.8 °C, 600 s, 21.4 °C) (163.0 °C, 168.0 °C) in a PS-PVME (50-50) mixture. (a) 60 s, (b) 120 s, (c) 240 s, (d) 480 s, (e) 720 s, and (f) 960 s after the second quench. The bar corresponds to 40 μm for (a)–(c), while to 20 μm for (d)–(f).

of the interface of the original droplets. It should be noted that the large, original domains also coarsen with time. Figure 2 shows phase separation in the same mixture caused by a double quench (2.8 °C, 2400 s, 21.8 °C) (163.0 °C, 168.0 °C). This pattern evolution is completely different from that observed in Fig. 1. This striking difference is likely caused by the small difference in ΔT_1 between the two quench conditions. In Fig. 2, the double-quench condition causes phase inversion phenomenon accompanying a complete reorganization of the phase-separated structure.

In polymer-polymer mixtures, we see only the rather early stage of a second phase separation before the large-scale exchange of materials over the original domains, because of slow dynamics in polymer mixtures. The overall pattern evolution caused by a double quench can be observed much easier in polymer-liquid mixtures than in polymer-polymer mixtures since the elementary diffusion process is much faster in the former than in the latter.

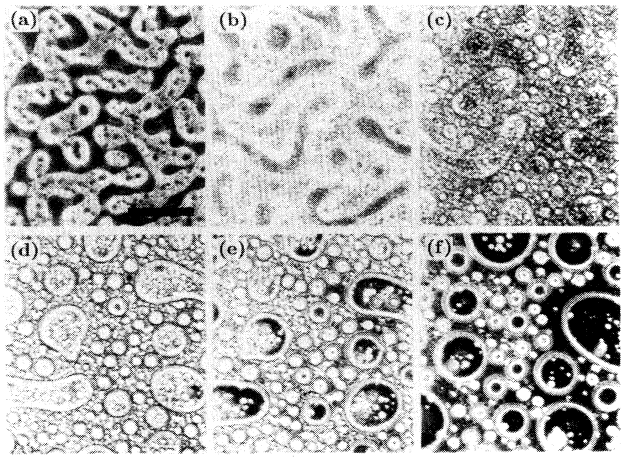

FIG. 2. Pattern evolution caused by a double quench (2.8 °C, 2400 s, 21.8 °C) (163.0 °C, 168.0 °C) in a PS-PVME (50-50) mixture. (a) 24 s, (b) 60 s, (c) 180 s, (d) 360 s, (e) 600 s, and (f) 1200 s after the second quench. The bar corresponds to 20 μm.

Thus we perform experiments also in a polymer solution. Figure 3 shows the pattern evolution caused by a double quench (0.3 °C, 600 s, 1.0 °C) (32.7 °C, 33.0 °C) in a PVME-water (5-95) mixture. The small domains newly appeared grow with time in both original droplets (PVME-rich phase) and matrix, and at the same time they disappear first from the interfacial region. Eventually, small droplets caused by a second quench completely disappear.

Next we describe the pattern evolution caused by a double quench composed of a first quench and a subsequent *shallower* quench within the two-phase region. Figure 4 shows pattern formation accompanied by such a quench (22.0 °C, 3600 s, 6.8 °C) (162.0 °C, 168.0 °C) in a PS-PVME (50-50) mixture. After the second quench, the interface first becomes very bright and thick [see Fig. 4(b)], and then the excess material in a droplet diffuses outward through the interface. The diffusion flow from PVME-rich droplets starts to overlap with each other and forms a high-PVME-concentration region having a bright contrast, in the middle of the matrix. During this process, we can clearly see the deformation of interface, or interface instability.

Pattern formation caused by double quenches can be discussed on the basis of a phase diagram. Possible double-quench experiments are shown in Fig. 5. Figure 5(a) shows various deeper second quenches in an asymmetric phase diagram. In an asymmetric phase diagram or under an off-critical quench condition, the two coexisting phases could be brought into different states of instability by a further deeper quench: One phase become metastable, while the other unstable (the case *b*). Under a certain condition, even phase inversion could be caused by a second quench as indicated in the case *d*; namely, a minority phase becomes a major phase, and vice versa.

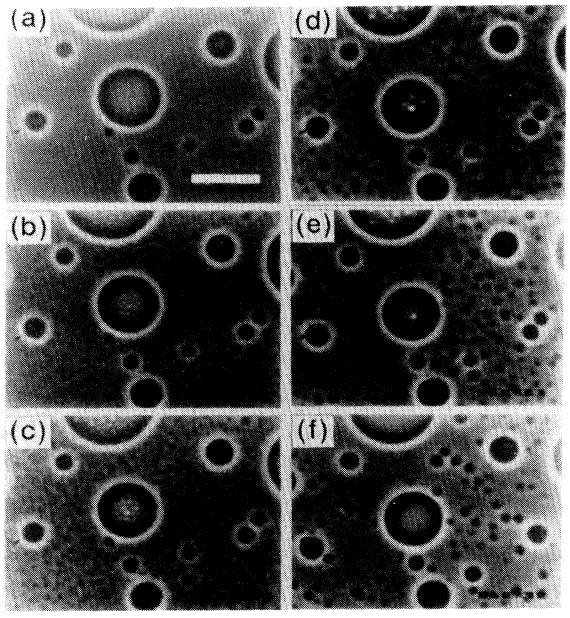

FIG. 3. Pattern evolution caused by a double quench (0.3 °C, 600 s, 1.0 °C) (32.7 °C, 33.0 °C) in a PVME-water (5-95) mixture. (a) 0.68 s, (b) 2.15 s, (c) 3.85 s, (d) 13.25 s, (e) 28.70 s, and (f) 50.01 s after the second quench. The bar corresponds to 40 μm.

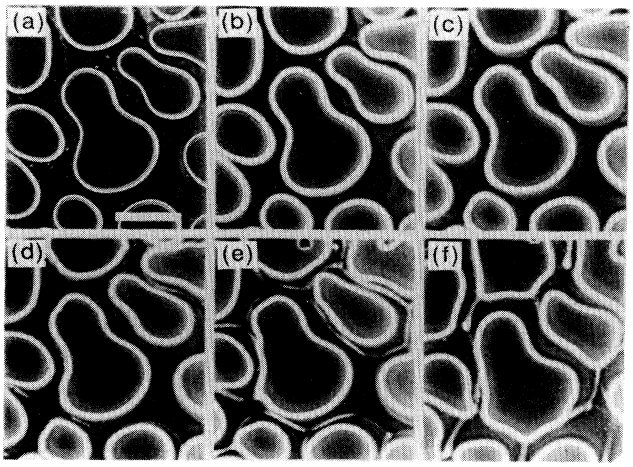

FIG. 4. Pattern evolution caused by a double quench (22.0 °C, 3600 s, 6.8 °C) (162.0 °C, 168.0 °C) in a PS-PVME (50-50) mixture. (a) −10 s, (b) 300 s, (c) 900 s, (d) 1500 s, (e) 3600 s, and (f) 9000 s after the second quench. The bar corresponds to 10 μm.

Such behavior is actually observed in Fig. 2, and there the original phase-separated structure is completely reorganized. This phenomenon would not happen under a symmetry-preserving quench, namely under a critical quench condition in a symmetric phase diagram. Figure 5(b) shows two kinds of shallower second quenches for a symmetric phase diagram: One is for a second quench within the two-phase region (the case *a*), while the other is for that into the one-phase region (the case *b*). In the latter the system simply relaxes to the homogeneous state, but in the former unusual pattern formation is observed in Fig. 4.

First we discuss the pattern evolution caused by a *deeper* double quench. When a deeper quench is performed in the initial or intermediate stage of phase separation after the first quench, the distribution of order parameter (concentration) may still be broad, and further the original phase-separated structure is not so large

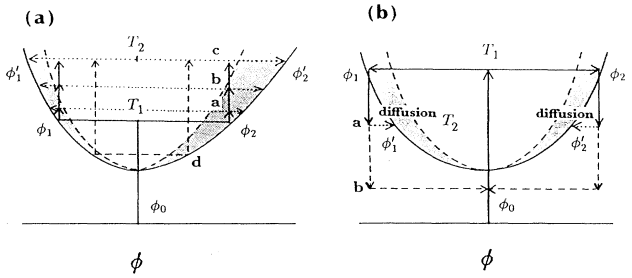

FIG. 5. (a) Various kinds of double-quench sequences consisting of a first deeper quench and a subsequent deeper quench. In case *a*, both phases become metastable. In case *b*, one phase becomes metastable, while the other unstable. In case *c*, both phases become unstable. In case *d*, phase inversion is induced by the second quench. (b) Two kinds of double-quench sequences consisting of a first deeper quench and a subsequent shallower quench. Cases *a* and *b* correspond to a second shallower quench into a two-phase region and into a one-phase region, respectively.

compared to the characteristic size of the second phase separation. Thus the original phase-separated structure would be almost completely destroyed and reorganized by a subsequent quench because of a strong diffusional coupling between original and subsequent phase separations.

For a double quench having a large Δt, the first phase separation enters into a late stage before a second deeper quench, and thus the two coexisting phases almost have equilibrium compositions of ϕ_1 and ϕ_2. By a second deeper quench, each of the phases further starts to separate into two phases, ϕ_1' and ϕ_2' [see Fig. 5(a)]. The initial stage of this second phase separation in the original phase having a composition of ϕ_i ($i=1$ or 2) should be similar to the phase separation of a homogeneous mixture having a composition of ϕ_i, caused by a single quench from T_1 to T_2. This is because in the initial stage phase separation proceeds almost independently in both original droplets and matrix. The coarsening dynamics in this stage is dominated by the Brownian coagulation [16,17] and the Lifshitz-Slyozov process [18,19]. Thus the two characteristic length scales for the large and small phase-separated structures, λ_1 and λ_2, grow as $\lambda_1 \sim t^{\alpha}$ and $\lambda_2 \sim (t-\Delta t)^{\alpha}$, respectively, for a small value of $(T_2-T_1)/T_1$. In our system, α was found to be $\frac{1}{3}$. For a large value of $(T_2-T_1)/T_1$, the behavior is much more complicated.

In the late stage, on the other hand, the two pattern evolutions with different spatial scales are strongly coupled with each other through the global diffusion between the original droplets and the matrix. The boundary between the initial independent growth to the strongly correlated growth locates around the time $\tau_R \sim R^2/D$, where R is the typical size of the original domains and D the diffusion constant. Reflecting this transition in the growth mechanism, the scattering peak intensity for λ_2 grows in the initial stage and then decays after the transition. In the late stage, the large curvature difference between the original interface and the small droplets leads to a difference in the boundary matrix composition. This causes the diffusion flow from the small droplets inside a large droplet to the original matrix and also from the small droplets in the matrix to the original droplets. Thus small droplets in both phases gradually evaporate from the neighbor of the original interface (see Fig. 3). For single-quench conditions, this mechanism is known as the evaporation-condensation mechanism (Lifshitz-Slyozov process) [18,19]. It should be noted that in the present case the sign of the interfacial curvature is different between the interacting small and large domains, while in usual phase separation it is the same. Finally, the structure formed by the double quench relaxes to the structure very close to the original one prior to the second quench, and then slowly coarsens (see Fig. 3). This is simply because the second quench is not so deep, and thus the final volume fraction is not so different from that for the initial one just before the second quench.

Next we discuss the pattern formation caused by a shallower quench. A shallower second quench causes pattern formation completely different from a deeper

second quench. After the second quench, a concentration adjustment is required at the boundary to establish local equilibrium [13]. This process is characterized by the time scale of $t_0 \sim \xi^2/D$ (ξ is the bulk correlation length), which is the time for material to diffuse across the interface thickness. On this time scale t_0, the concentration gradient $d\phi/dz$ is established around the interface. Since the measure of supercooling $\delta\phi$ is given by $\delta\phi = \phi_1' - \phi_1 = \theta(\phi_1' - \phi_2') = \theta\Delta\phi$ [see Fig. 5(b)], $d\phi/dz$ can be estimated as $\sim\theta\Delta\phi/\xi$. Accordingly, the depletion layer characterized by a macroscopic supercooling length of $\sim\xi/\theta$ is formed. This depletion layer likely causes an optical diffraction effect, and thus the interface becomes very bright just after the second quench [see Fig. 4(b)]. Then the diffusion flow caused by the concentration imbalance across the interface carries the excess component from each droplet to the surrounding matrix isotropically [see Fig. 4(c)]. During this process, the flow coming from each droplet starts to overlap with each other in the middle of the matrix [see Fig. 4(d)]. This again causes the region to have excess components, and accordingly a new nonequilibrium state. Then the redistribution of concentration further proceeds to establish a final equilibrium. Since the contribution of the volume part to the free energy is much larger than that of the interface part, the volume ratio between the two phases first approaches its final one at the expense of the incorrect local volume-surface ratio. This imbalance and the resulting diffusion field between the droplets and the regions having excess PVME components causes the droplet deformation, namely a kind of interface instability [see Fig. 4(e) and (f)]. Up to this stage, the initial droplet distribution just before the second quench strongly affects the pattern formation, as observed in Fig. 4. Finally the shape relaxation occurs very slowly to reduce the total interfacial energy. This process accompanies the complete reorganization of droplet shape and droplet distribution, since the incorrect local volume-surface ratio can be removed only by the large-scale diffusion. However, since the driving force coming from the interface energy is too weak for a quick, large-scale reorganization, this final process is likely very slow.

It should be noted that this large-scale interface instability occurs only for a shallower second quench within the two-phase region. For a second shallower quench to the one-phase region, the system becomes homogeneous by a simple diffusion between the two coexisting phases, since in this case a local equilibrium concentration at the interface is equal to the average concentration and is always consistent with the final equilibrium concentration. Even for a second shallower quench in the two-phase region, the interface instability would never appear under critical quench conditions for a symmetric phase diagram.

In summary, double quenches within the two-phase region are found to cause interesting pattern formation. Variation of Δt, ΔT_1, and ΔT_2 leads to various kinds of pattern evolution. Theoretically, this is a problem to solve the time-dependent Ginzburg-Landau equation under double-quench conditions. However, the problem is not so simple because of the nonlocal nature of the equation. Thus further experimental and theoretical studies are necessary for the full understanding of the pattern evolution caused by complex quenches. A double quench is one of the simplest multiple quenches including a periodic quench, and thus probably becomes a good starting point to understand the relaxation of a nonequilibrium state to perturbations, especially within a metastable or unstable region. A double-quench experiment also provides us with a possibility of morphology control of polymer blends and alloys. Here we demonstrate the qualitative nature of phase separation accompanied by double quenches. The details including more quantitative analysis of pattern evolution by a digital image analysis will be published elsewhere.

This work was partly supported by a Grant-in-Aid from the Ministry of Education, Science, and Culture, Japan, a grant from Kanagawa Academy of Science and Culture, and a grant from Iketani Foundation of Science and Technology.

[1] J. D. Gunton *et al.*, in *Phase Separation and Critical Phenomena,* edited by C. Domb and J. H. Lebowitz (Academic, London, 1983), Vol. 8.
[2] *Dynamics of Ordering Process in Condensed Matter,* edited by S. Komura and H. Furukawa (Plenum, New York, 1987).
[3] H. Tanaka *et al.*, Phys. Rev. Lett. **65**, 3136 (1990).
[4] K. Binder, Phys. Rev. B **15**, 4425 (1977).
[5] N. C. Wong and C. M. Knobler, Phys. Rev. Lett. **43**, 1733 (1979); **45**, 498 (1979).
[6] N. C. Wong and C. M. Knobler, J. Chem. Phys. **69**, 725 (1978).
[7] R. Ruiz, Phys. Rev. A **26**, 2227 (1982).
[8] A. Onuki, Prog. Theor. Phys. **66**, 1230 (1981).
[9] A. Onuki, Phys. Rev. Lett. **48**, 753 (1982).
[10] A. Onuki, Prog. Theor. Phys. **67**, 768 (1982); **67**, 787 (1982); **67**, 1740 (1982).
[11] M. Joshua *et al.*, Phys. Rev. Lett. **54**, 1175 (1985).
[12] D. Beysens and F. Perot, J. Phys. (Paris) Lett. **45**, L31 (1984).
[13] D. Jasnow *et al.*, Phys. Rev. A **23**, 3192 (1981).
[14] H. Tanaka, Polym. Prep. Jpn. **40**, 766 (1991).
[15] M. Okada *et al.*, Polym. Prep. Jpn. **40**, 767 (1991).
[16] K. Binder and D. Stauffer, Phys. Rev. Lett. **33**, 1006 (1974).
[17] K. Binder and D. Stauffer, Adv. Phys. **25**, 343 (1976).
[18] I. M. Lifshitz and V. V. Slyozov, J. Phys. Chem. Solids **19**, 35 (1961).
[19] C. Wagner, Z. Elektrochem. **65**, 581 (1961).

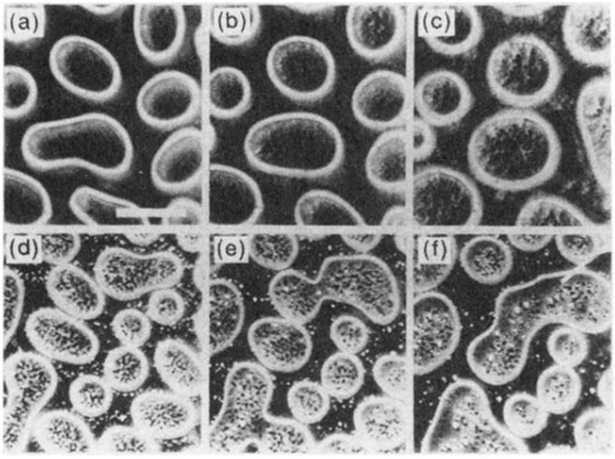

FIG. 1. Pattern evolution caused by a double quench (6.8 °C, 600 s, 21.4 °C) (163.0 °C, 168.0 °C) in a PS-PVME (50-50) mixture. (a) 60 s, (b) 120 s, (c) 240 s, (d) 480 s, (e) 720 s, and (f) 960 s after the second quench. The bar corresponds to 40 μm for (a)–(c), while to 20 μm for (d)–(f).

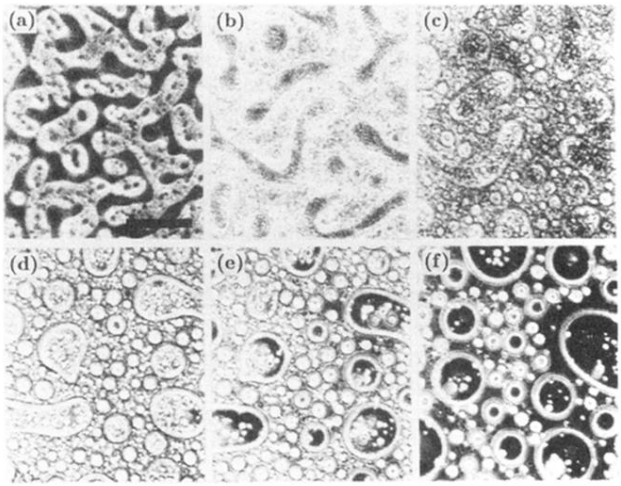

FIG. 2. Pattern evolution caused by a double quench (2.8 °C, 2400 s, 21.8 °C) (163.0 °C, 168.0 °C) in a PS-PVME (50-50) mixture. (a) 24 s, (b) 60 s, (c) 180 s, (d) 360 s, (e) 600 s, and (f) 1200 s after the second quench. The bar corresponds to 20 μm.

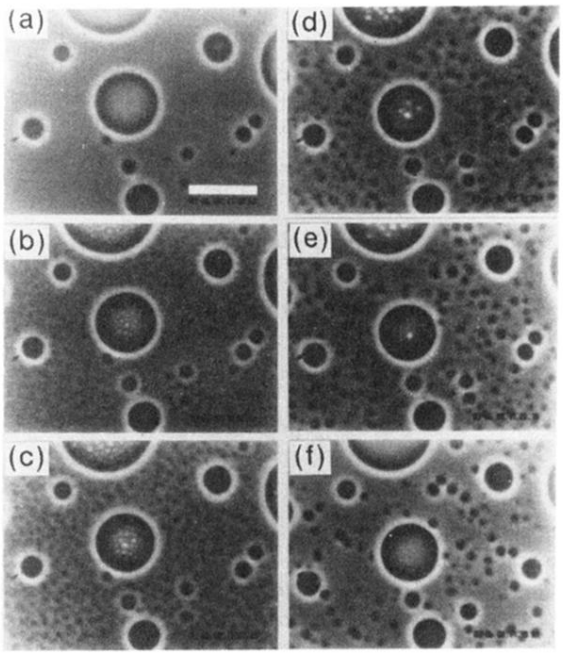

FIG. 3. Pattern evolution caused by a double quench (0.3 °C, 600 s, 1.0 °C) (32.7 °C, 33.0 °C) in a PVME-water (5-95) mixture. (a) 0.68 s, (b) 2.15 s, (c) 3.85 s, (d) 13.25 s, (e) 28.70 s, and (f) 50.01 s after the second quench. The bar corresponds to 40 μm.

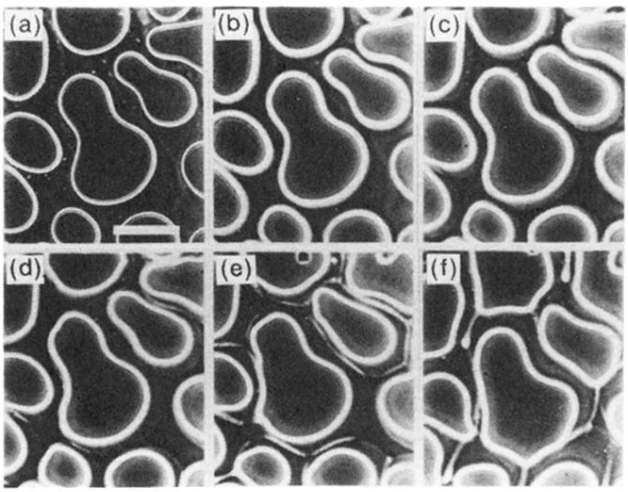

FIG. 4. Pattern evolution caused by a double quench (22.0 °C, 3600 s, 6.8 °C) (162.0 °C, 168.0 °C) in a PS-PVME (50-50) mixture. (a) −10 s, (b) 300 s, (c) 900 s, (d) 1500 s, (e) 3600 s, and (f) 9000 s after the second quench. The bar corresponds to 10 μm.